



Published in final edited form as:

*Macromol Biosci.* 2012 April ; 12(4): 502–514. doi:10.1002/mabi.201100350.

## Targeting of Multidrug-Resistant Human Ovarian Carcinoma Cells With Anti-P-Glycoprotein Antibody Conjugates

Kirk D. Fowers and

Department of Bioengineering, University of Utah, Salt Lake City, UT 84112, USA

Jindrich Kopeček

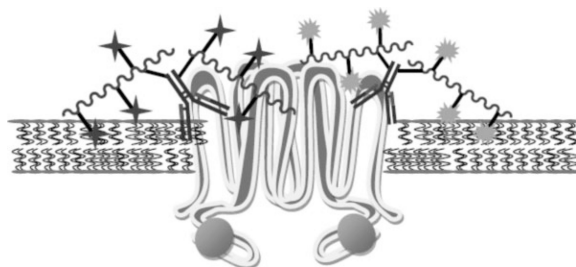
Department of Bioengineering, University of Utah, Salt Lake City, UT 84112, USA

Department of Pharmaceutics and Pharmaceutical Chemistry, University of Utah, Salt Lake City, UT 84112, USA

Jindrich Kopeček: jindrich.kopecek@utah.edu

### Abstract

A monoclonal antibody (mAb) to P-glycoprotein (Pgp), UIC2, is used as a targeting moiety for *N*-(2-hydroxypropyl)methacrylamide (HPMA) copolymer/drug [(meso chlorin  $e_6$  mono(*N*-2-aminoethylamide) (Mce $_6$ ) or doxorubicin (DOX)] conjugates to investigate their cytotoxicity towards the Pgp-expressing human ovarian carcinoma cell line A2780/AD. The binding, internalization, and subcellular trafficking of a fluorescein labeled UIC2 targeted HPMA copolymer are studied and show localization to the plasma membrane with limited internalization. The specificity of the UIC2-targeted HPMA copolymer/drug conjugates are confirmed using the sensitive cell line A2780 that does not express Pgp.



### Keywords

anti-P-glycoprotein antibodies; doxorubicin; HPMA copolymers; mesochlorin  $e_6$ ; ovarian carcinoma

### 1. Introduction

The development of multidrug resistance (MDR) toward a broad range of compounds following administration of a single anti-cancer agent is one of the major obstacles in cancer chemotherapy.<sup>[1–4]</sup> As one of the primary mechanisms involved in MDR induction, overexpression of the *MDR1* gene can be responsible for increased levels of the transmembrane protein P-glycoprotein (Pgp). Increased Pgp expression is an integral

property of both normal cell function and in cancer cells, which develop MDR as a result of exposure to Pgp substrates.<sup>[5]</sup> Pgp, also designated as ABCB1, is an ATP-dependent pump that recognizes a wide array of chemical structures and is a member of the ATP-Binding Cassette (ABC) superfamily.<sup>[1,6,7]</sup> Pgp effluxes a variety of drug classes, including chemotherapeutic agents, and its expression is often associated with a poorer outcome in cancer patients.<sup>[8,9]</sup> Alternative methods for treating MDR cancers are actively being sought to improve the efficacy of anti-cancer agents.

Polymer/drug conjugates based on *N*-(2-hydroxypropyl)-methacrylamide (HPMA) copolymers have been shown to reduce both the systemic toxicity of free drugs and increase drug accumulation in solid tumors *in vivo*.<sup>[10–12]</sup> The use of HPMA copolymer/drug conjugates as potential treatments for solid tumors has been extensively studied.<sup>[11]</sup> The increased accumulation of macro molecules in solid tumors, attributed to an increased vascular permeability and the absence of a lymphatic drainage system, is termed the enhanced permeability and retention (EPR) effect.<sup>[13,14]</sup> HPMA copolymer/drug conjugates have been shown to alter the delivery mechanism and ultimate target of anti-cancer agents to MDR cell lines versus standard chemotherapy where the diffusion of small molecular weight drugs into the cell may be excreted by transmembrane pumps such as Pgp.<sup>[15–19]</sup> The cytotoxicity of HPMA copolymer/ drug conjugates to a variety of cell models has been further enhanced by targeting over-expressed antigen on tumor cells, and is one means to target cells over-expressing Pgp.<sup>[20–23]</sup> Macromolecules targeted by a monoclonal antibody (mAb) have three possible fates once they bind to an antigen on the cell surface, (1) receptor mediated pinocytosis triggering localization in the lysosomal compartment, (2) prolonged localization at the plasma membrane (PM) followed by internalization, and (3) localization at the PM due to limited internalization or efficient recycling as found for antibodies to Pgp.<sup>[24–29]</sup> In order to examine localization and targeting to over-expressed Pgp in a MDR carcinoma phenotype, an anti-Pgp mAb, UIC2, was covalently attached to HPMA copolymer/drug conjugates.

The development of antibodies to Pgp has created opportunities to counteract MDR by incorporating antibodies, i.e., UIC2 into HPMA copolymer/drug conjugates, which have the potential to specifically target Pgp.<sup>[30–33]</sup> UIC2 targeted and non-targeted HPMA copolymer/ drug conjugates were synthesized containing non-degradable (glycine, G or glycyglycine, GG) or intralysosomally degradable (glycylphenylalanylleucylglycine, GFLG) spacers and their cytotoxicity towards a MDR, A2780/AD, or sensitive, A2780, human ovarian carcinoma cell line was studied. In addition to the degradable or non-degradable nature of the linker, the composition of the linker may also play a part in determining the conjugates cytotoxicity.<sup>[19,34]</sup> Examining the effects of G, GG, or GFLG spacers on the cytotoxicity of UIC2 targeted HPMA copolymer/drug conjugates will further our understanding of methods to combat the development of MDR in carcinoma cells where the HPMA copolymer/drug conjugate remain predominantly localized to the PM as a result of binding to Pgp. [6,8,24–28]

Aims of this study included determining the localization of UIC2 targeted HPMA copolymer conjugates labeled with fluorescein, the specificity and cytotoxicity of UIC2 targeted HPMA copolymer/drug conjugates containing meso chlorin e<sub>6</sub> mono (*N*-2-

aminoethylamide) (Mce<sub>6</sub>) or doxorubicin (DOX), and the influence of the structure of the drug spacer (GFLG vs. G or GG) towards the Pgp-expressing, MDR human ovarian carcinoma cell line A2780/AD.

## 2. Experimental Section

### 2.1. Cell Lines

Human ovarian carcinoma cell lines A2780, DOX sensitive, and A2780/AD, DOX resistant, were obtained from Dr. T. C. Hamilton (Fox Chase Cancer Center, PA). The A2780/AD cell line expresses Pgp due to previous exposure to DOX.<sup>[35]</sup> A2780 and A2780/AD cells were cultured in Roswell Park Memorial Institute (RPMI) 1640 medium containing  $10 \mu\text{g} \cdot \text{mL}^{-1}$  insulin, supplemented with 10% fetal bovine serum (FBS). Experiments were conducted on cells in the exponential growth phase. The hybridoma cell line that produces the IgG<sub>2a</sub> mAb to P-glycoprotein (UIC2) was purchased from ATCC (Rockville, MD). Cells were kept at 37 °C in a humidified atmosphere containing 5% CO<sub>2</sub> (v/v).

### 2.2. Antibody Production

UIC2 hybridoma cells were reduced from Dulbecco's modified Eagle Medium (DMEM) containing 10% fetal bovine serum by serial dilution to 1.25% FBS and then to serum-free medium Hybridoma-SFM (Gibco Life Sciences). Cells were then seeded into a Cellco Bioreactor system. The UIC2 antibody was harvested every 24 h and purified by affinity chromatography (Gammabind Plus Sepharose, Pharmacia).<sup>[36]</sup> The purity of the antibody was assessed by sodium dodecylsulfate/polyacrylamide gel electrophoresis (SDS-PAGE).

### 2.3. Labeling of UIC2 Antibody

Free mAb was radiolabeled using the Iodogen method. The mAb, 0.29 mg, in Dulbecco's phosphate-buffered saline (DPBS) pH = 7.4 and 10  $\mu\text{L}$  (0.5 mCi) of Na<sup>125</sup>I were mixed in a glass test tube containing an Iodogen film. The reaction mixture was incubated for 20 min with periodic stirring. The unbound <sup>125</sup>I was separated from the labeled mAb using two passages over a PD-10 column (Pharmacia) equilibrated in DPBS containing 0.5% BSA. The labeled mAb was stored at 4°C.

### 2.4. Affinity Constant of UIC2

The affinity constant,  $K_a$ , of UIC2 for Pgp was determined using A2780/AD cells. Non-specific binding of radiolabeled UIC2 was measured using the A2780 cell line, which does not express Pgp. Cells were suspended following trypsinization in 1 mL Hank's balanced salt solution (HBSS) containing 0.5% bovine serum albumin (BSA) and  $5 \times 10^6$  cells. Unlabeled UIC2 was mixed with equivalent amounts of <sup>125</sup>I labeled UIC2 and diluted between 0.08 and  $20 \mu\text{g} \cdot \text{mL}^{-1}$ . The cells were incubated with UIC2 for 5.5 h at 4°C on a rotating sample holder. The cells were centrifuged and the supernatant was aspirated. The cells were then counted using a  $\gamma$ -counter. The amount bound to the A2780 cell line, due to non-specific binding, was subtracted from the value for the A2780/AD cell line. A Scatchard plot was used to obtain  $K_a$ .

## 2.5. Synthesis of HPMA Copolymer/Drug Conjugates

Polymeric precursors were prepared by radical copolymerization of HPMA with *N*-methacryloylglycine *p*-nitrophenyl ester (MA-G-ONp),<sup>[37,38]</sup> to obtain P-G-ONp; with *N*-methacryloylglycylglycine *p*-nitrophenyl ester (MA-GG-ONp), to obtain P-GG-ONp; and with *N*-methacryloylglycylphenylalanylleucylglycine *p*-nitrophenyl ester (MA-GFLG-ONp),<sup>[39]</sup> to obtain P-GFLG-ONp; and with MA-G-ONp and 5-[3-(methacryloylaminopropyl)thioureidyl] fluorescein (MA-AP-FITC),<sup>[40]</sup> to obtain polymer precursor 6 [P-(AP-FITC)-ONp], using 2,2'-azoisobutyronitrile as the initiator, in acetone at 50 °C as previously described.<sup>[38]</sup>

The *p*-nitrophenyl (ONp) content was determined by UV spectroscopy using  $\epsilon_{272} = 9500$  in dimethyl sulfoxide (DMSO) containing 1% acetic acid. The molecular weight of HPMA copolymer precursors was estimated, following aminolysis with 1-amino-2-propanol, by size-exclusion chromatography on a Superose 6 column (Pharmacia, HR10/30) calibrated with fractions of poly(HPMA).

Mce<sub>6</sub> and DOX were attached to HPMA copolymer precursors by partial aminolysis of ONp groups to yield the following polymeric precursors; polymer precursor **1** [P-(G-Mce<sub>6</sub>)-ONp], **2** [P-(GG-Mce<sub>6</sub>)-ONp], **3** [P-(GFLG-Mce<sub>6</sub>)-ONp], **4** [P-(GG-DOX)-ONp], and **5** [P-(GFLG-DOX)-ONp].<sup>[41]</sup> The polymer precursors were separated from free drug on an LH-20 column equilibrated in methanol containing 1% acetic acid. The ONp and drug content were determined spectrophotometrically as previously described.<sup>[41]</sup> Polymer precursors **1**, **2**, **3**, **4**, and **5** were subsequently divided into two parts. The first part was aminolyzed with an excess of 1-amino-2-propanol to obtain conjugates **1** [P-(G-Mce<sub>6</sub>)], **2** [P-(GG-Mce<sub>6</sub>)], **4** [P-(GFLG-Mce<sub>6</sub>)], **6** [P-(GG-DOX)], and **8** [P-(GFLG-DOX)]. The second fraction was dissolved in dimethylformamide ( $\approx 20\text{wt}\%$ ) and added dropwise to a solution of UIC2 (10 mg · mL<sup>-1</sup>) in phosphate-buffered saline (PBS) at pH = 7.2 while stirring. The reaction proceeded for 2 h at room temperature (RT), and the pH was gradually increased with 0.1 M NaOH to 9.0 over a 2h period. The mAb targeted HPMA copolymer/drug conjugates were purified by size exclusion chromatography on a Superose 6 preparative (Pharmacia, HR 16/ 60) column and fractions corresponding to the conjugate were collected based on spectral, refractometric and protein detection methods. Conjugate fractions were pooled, concentrated, and characterized for the polymer content (based on drug adsorption) and protein content [bicinchoninic acid (BCA) assay]. The copolymers were designated as conjugates **3** [P-(GG-Mce<sub>6</sub>)-mAb], **5** [P-(GFLG-Mce<sub>6</sub>)-mAb], **7** [P-(GG-DOX)-mAb], and **9** [P-(GFLG-DOX)-mAb].

Polymer precursor **6** [P-(AP-FITC)-ONp] was either aminolyzed with 1-amino-2-propanol and designated as conjugate **10** [P-(AP-FITC)] or subsequently reacted with UIC2 to obtain conjugate **11** [P-(AP-FITC)-mAb]. The P refers to the HPMA copolymer backbone as shown in Table 1.

The Mce<sub>6</sub>, DOX, and fluorescein contents of individual copolymers were evaluated by UV spectroscopy. The extinction coefficients used (in L · mol<sup>-1</sup> · cm<sup>-1</sup>) were as follows: Mce<sub>6</sub>,  $\epsilon_{394} = 1.58 \times 10^5$  in methanol or  $\epsilon_{394} = 1.07 \times 10^5$  in water; DOX,  $\epsilon_{490} = 1.1 \times 10^4$  in water; and fluorescein;  $\epsilon_{490} = 8.0 \times 10^4$  in 0.1 M borate pH = 9.3 buffer.

Protein content was determined by BCA assay (Pierce). Contribution to the protein content from the HPMA copolymer/ drug conjugate was determined using individual, matched aminolyzed HPMA copolymer/drug conjugate precursors. The levels measured were subtracted from the amount determined for each targeted HPMA copolymer/drug conjugate. Briefly, standard curves were constructed using serial dilutions of a  $2 \text{ mg} \cdot \text{mL}^{-1}$  stock solution of HPMA copolymer/drug conjugates or UIC2. The concentration of the HPMA copolymer in UIC2 targeted HPMA copolymer/drug conjugates was determined by measuring the concentration of the drug, and subtracting the corresponding absorbance contribution to the BCA assay as determined from the standard curve. The chemical structure of the conjugates is shown in Figure 1. Their characterization is listed in Table 2.

## 2.6. Internalization of Conjugates

Cells were plated on  $25 \times 25 \text{ mm}^2$  glass coverslips in 6-well plates at a density of  $2 \times 10^5$  cells perwell and incubated for 24h.RPMI-1640 media containing the fluorescein labeled copolymer,  $150 \text{ } \mu\text{g} \cdot \text{mL}^{-1}$ , P-(AP-FITC)-mAb, P-(AP-FITC), and unlabeled mAb ( $10 \mu\text{g} \cdot \text{mL}^{-1}$ ) were added to the individual wells and incubated at  $4 \text{ }^\circ\text{C}$  to observe saturation of cell surface Pgp and at  $37 \text{ }^\circ\text{C}$  to observe internalization and localization of conjugate **10** [P-(AP-FITC)], conjugate **11** [P-(AP-FITC)-mAb], or free mAb. Free mAb was visualized following a 30 min incubation of fluorescein labeled goat anti-mouse IgG ( $0.5 \text{ mg} \cdot \text{mL}^{-1}$ ).

The localization of conjugates **10** [P-(AP-FITC)] and **11** [P-(AP-FITC)-mAb], and UIC2 visualized with goat anti-mouse fluorescein labeled secondary mAb were determined on a Bio-Rad MRC 600 laser scanning confocal imaging system. The system is based on a Zeiss Axioplan microscope and a krypton-argon laser. The plan-apo objective ( $60 \times$ , numerical aperture 1.4, oil) was used. The images were obtained using a block of filters, excitation at 488 nm and emission through a 515 nm barrier filter. Following growth of the cells and incubation with conjugate **10** [P-(AP-FITC)], conjugate **11** [P-(AP-FITC)-mAb], or free mAb, coverslips were washed  $5 \times$  with DPBS followed by fixation of cells with 3% paraformaldehyde in DPBS for 20 min at RT. Coverslips were then prepared for mounting on a microscope slide using the SlowFade Light Antifade Kit (Molecular Probes).

## 2.7. Flow Cytometry

One million cells were trypsinized, pelleted by centrifugation, and suspended in Hank's balanced salt solution (HBSS)  $\text{pH} = 7.5$  containing 0.5% bovine serum albumin (BSA) and  $10 \text{ } \mu\text{g} \cdot \text{mL}^{-1}$  UIC2 for 30 min at  $4^\circ\text{C}$ . Cells were subjected to centrifugation and the supernatant aspirated and the pellet washed with DPBS containing 0.5% BSA. After an additional centrifugation, cells were suspended in HBSS with 0.5% BSA containing  $0.5 \text{ } \mu\text{g} \cdot \text{mL}^{-1}$  fluorescein isothiocyanate (FITC)-labeled goat anti-mouse IgG for 30min at  $4^\circ\text{C}$  followed by washing in DPBS containing 0.5% BSA and resuspension in DPBS containing 0.5% BSA as above. All solutions and incubations were maintained at  $4^\circ\text{C}$ . Cells were examined on a flow cytometer (Becton Dickenson FacScan) using the FL1 channel for fluorescein. Similar profiles were generated utilizing the fluorescein-labeled conjugate **11** [P-(AP-FITC)-mAb] and a modified protocol. Conjugate **11** [P-(AP-FITC)-mAb] was incubated as described above, except the concentration of the conjugate was  $100 \text{ } \mu\text{g} \cdot \text{mL}^{-1}$  of the mAb and the FITC-labeled goat anti-mouse IgG incubation step was omitted.

## 2.8. Cytotoxicity Bioassay

The inhibitory concentration at which 50% (IC<sub>50</sub>) of cell growth is inhibited relative to control cells was determined using a modified 3-(4,5-dimethylthiazol-2-yl)-2,5-diphenyltetrazolium bromide (MTT) cell survival bioassay.<sup>[42]</sup> Briefly, 10 000 A2780 or 20 000 A2780/AD cells were seeded in individual wells of a 96 well plate and incubated 24 h under cell culture conditions. Varying concentrations of free drug or HPMA copolymer/drug conjugates in RPMI-1640 medium were added to each well, with control cells receiving sterile DPBS.

For free Mce<sub>6</sub> and HPMA copolymer/Mce<sub>6</sub> conjugates, the cells were incubated with varying drug concentrations for 16 h under cell culture conditions. Then the drug solution was removed, fresh media added, and the cells were irradiated (3.0 mW cm<sup>-2</sup>) for 30min using a tungsten halogen light source filtered via a 650 nm bandpass filter and incubated an additional 72 h under cell culture conditions. For free DOX and HPMA copolymer/DOX conjugates, the cells were incubated with varying drug concentrations for 72 h under cell culture conditions. After the 72 h incubation for both Mce<sub>6</sub> and DOX protocols, the medium was replaced with 100 μL of fresh media and 25 mL of MTT (5 mg mL<sup>-1</sup>) in DPBS was added. Following a 4h incubation cells were dissolved in 100 μL of 50 vol% dimethylformamide in water containing 20% (w/v) sodium dodecylsulfate. The plates were incubated overnight and the absorbance read at 570 nm with a background correction at 630 nm. Mce<sub>6</sub> concentrations versus cell viability curves were constructed assuming control cells as 100% viable. Linear regression of Mce<sub>6</sub> concentration versus cell viability was performed to determine the IC<sub>50</sub>. The following formula for cell viability (V) was utilized to obtain the IC<sub>50</sub> for cells exposed to DOX:

$$V = \frac{Y - Y_0}{Y_m - Y_0} = \left(1 + \frac{C}{C_0}\right)^{-1} \quad (1)$$

where  $Y = Y_0 + \frac{Y_m - Y_0}{1 + C/C_0}$  and C<sub>0</sub> is the IC<sub>50</sub> dose, Y the optical density in a well-containing drug concentration C, Y<sub>m</sub> the optical density in a well with 100% cell viability, and Y<sub>0</sub> the optical density in a well with 0% cell viability.<sup>[43]</sup>

## 2.9. Determination of Cell-Associated Mce<sub>6</sub> Concentration

Cell associated Mce<sub>6</sub> was determined following incubation of the A2780/AD cells with the IC<sub>50</sub> dose determined in the cytotoxicity bioassay. The cells were plated and incubated with the IC<sub>50</sub> dose for 16 h, the drug solution was removed, and individual wells in 96 well plates were washed twice with 100mL DPBS and aspirated. The cells were then incubated with 100 mL stripping buffer at 4 8C for 5 min on a rocking sample holder.<sup>[44]</sup> The stripping buffer was collected and the cells were dissolved with 50 mL 1M NaOH overnight. The fluorescence of the solutions was measured using a photon counting spectrofluorometer PC-1 (ISS, Champaign, Il). The excitation wavelength was 394nm and the fluorescence emission was 636 and 645 nm for the stripping buffer and 1 M NaOH, respectively. Mce<sub>6</sub> standards from 0 to 50 nM were used to calculate the concentration in the stripping buffer and 1 M NaOH solutions. The stripping buffer was utilized since it is capable of dissociating



protein/protein interactions, but the contributions to the total fluorescence were minimal. However, the dissociation of non-targeted HPMA copolymer/Mce<sub>6</sub> conjugates from the cell surface due to the stripping buffer was incomplete. Therefore, the values from both solutions were combined and expressed as cell associated Mce<sub>6</sub>. Fluorescent intensity was normalized to the amount of cell protein using the Micro BCA assay (Pierce).

### 2.10. Statistics

All values report the mean  $\pm$  standard deviation unless otherwise noted. Statistical analysis was carried out utilizing the Pearson's correlation coefficient and Student's t-test;  $p < 0.05$  was considered statistically significant.

## 3. Results

### 3.1. Characterization of UIC2 Binding to A2780/AD Cells

The specificity of UIC2 for Pgp expressed on A2780/AD cells was demonstrated using flow cytometry (Figure 2). Marked shifts to the right were demonstrated for both the free mAb as well as conjugate **11** [P-(AP-FITC)-mAb] indicating the mAb conjugated to HPMA copolymer conjugate maintains recognition of Pgp and localization at the PM. To quantify the affinity of UIC2 for Pgp expressed on A2780/AD cells, the affinity constant,  $K_a$ , was determined from a Scatchard plot and was  $1.1 \times 10^8 \text{ L} \cdot \text{mol}^{-1}$ . Saturation of Pgp sites by UIC2 on A2780/AD cells was reached at  $20 \mu\text{g} \cdot \text{mL}^{-1}$ , similar to values cited in the literature.<sup>[45]</sup>

### 3.2. Localization of HPMA Copolymer/FITC Conjugates

Localization and/or intracellular trafficking of polymeric drug delivery systems are important consideration for the cytotoxic activity of anti-cancer drugs. Cytotoxicity is a function of cellular localization and the composition of the spacer utilized to attach the anti-cancer agent.<sup>[19,34]</sup> The localization and internalization of conjugate **10** [P-(AP-FITC)], and conjugate **11** [P-(AP-FITC)-mAb], which contained non-degradable spacers, were incubated with A2780/AD cells and monitored using confocal fluorescence microscopy and compared to UIC2. UIC2 incubated with A2780/AD cells at 4°C for 16 h exhibited PM localization due to temperature-induced inhibition of pinocytosis (Figure 3A). Incubation at 37°C also showed PM localization, but also exhibited limited internalization (Figure 3B), which is likely due to Pgp presence in early endosomes, which may function as an intracellular reserve, and to a lesser extent in lysosomes.<sup>[6,24–27]</sup> Incubation of conjugate **11** [P-(AP-FITC)-mAb] at 4 and 37°C showed similar profiles (Figure 3C and D).<sup>[28]</sup> While the pattern of fluorescence was similar, conjugate **11** [P-(AP-FITC)-mAb] exhibited a more intense localized pattern within the cell than UIC2 (compare Figure 3B with Figure 3D). Cells incubated for up to 48 h with conjugate **11** [P-(AP-FITC)-mAb] showed similar cellular fluorescence as noted at 16 h, which may indicate limited internalization of conjugate **11** [P-(AP-FITC)-mAb], Pgp complexes (Figure 3E).<sup>[6,24–28]</sup>

In contrast, incubation of conjugate **10** [P-(AP-FITC)] for 16 h with A2780/AD cells exhibited lysosomal uptake, as noted for fluorescence in the perinuclear region (Figure 3F).

Conjugate **10** [P-(AP-FITC)] had negligible fluorescence at 4°C due to minimal adsorption to the cell membrane of the hydrophilic copolymer (data not shown).

### 3.3. Cytotoxicity of HPMA Copolymer/Drug Conjugates

Examination of the cytotoxicity of HPMA copolymer/drug conjugates was performed for the following reasons: (1) to compare the efficiency to inhibit cell growth of the various forms of drug in the A2780 and A2780/AD cell lines, (2) to determine the effect of non-degradable (G or GG) and degradable (GFLG) spacers on the concentration required to inhibit cell growth, (3) to examine differences in the cytotoxicity of Mce<sub>6</sub> and DOX towards A2780 and A2780/AD cell lines, (4) to compare the effectiveness of mAb targeting to reduce the IC<sub>50</sub> over non-targeted HPMA copolymer/drug conjugates in A2780/AD cells, and (5) to demonstrate the specificity of the mAb for Pgp expressing cells.

The IC<sub>50</sub> doses for HPMA copolymer/drug conjugates and free drugs are listed in Table 3. The dose dependent inhibition of cell growth is shown in Figure 4 for free Mce<sub>6</sub> and HPMA copolymer-Mce<sub>6</sub> conjugates. The free drug exhibits a higher cytotoxicity in vitro than HPMA copolymer-Mce<sub>6</sub> conjugates drug for A2780 and A2780/AD cells due to the difference in the uptake mechanism, diffusion for free drug, pinocytosis for non-targeted HPMA copolymer/drug conjugates, and primarily PM localization on A2780/AD cells for UIC2 targeted HPMA copolymer/drug conjugates.<sup>[24–28,39]</sup>

The cytotoxicity of HPMA copolymer/drug conjugates increased when the drug was attached via a degradable spacer, GFLG, as in conjugate **4** [P-(GFLG-Mce<sub>6</sub>)], conjugate **8** [P-(GFLG-DOX)], conjugate **5** [P-(GFLG-Mce<sub>6</sub>-mAb)], and conjugate **9** [P-(GFLG-DOX-mAb)], when compared to conjugates containing non-degradable spacers, G or GG, for conjugate **1** [P-(G-Mce<sub>6</sub>)], conjugate **2** [P-(GG-Mce<sub>6</sub>)], conjugate **3** [P-(GG-Mce<sub>6</sub>-mAb)], conjugate **6** [P-(GG-DOX)], and conjugate **7** [P-(GG-DOX-mAb)], respectively, for A2780 and A2780/AD cells, as noted for other targeted and non-targeted HPMA copolymers.<sup>[19,23,34]</sup> Release of the drug from internalized HPMA copolymer/drug conjugates can occur due to enzymatic cleavage between the GFLG spacer, a cathepsin B substrate, and the drug once the conjugate has been internalized and reaches the lysosomal compartment.<sup>[46,47]</sup> Increased cytotoxicity, likely following release of the drug in the lysosomal compartment, from the GFLG spacer was more pronounced for conjugate **4** [P-(GFLG-Mce<sub>6</sub>)] versus conjugate **2** [P-(GG-Mce<sub>6</sub>)], than conjugate **8** [P-(GFLG-DOX)] versus conjugate **6** [P-(GG-DOX)], for both A2780 and A2780/AD cell lines. The IC<sub>50</sub> of conjugate **4** [P-(GFLG)-Mce<sub>6</sub>] conjugate was similar to free Mce<sub>6</sub> for both the A2780 and A2780/AD cell lines as shown in Table 3.

Non-targeted HPMA copolymer-Mce<sub>6</sub> conjugates exhibited no statistically significant difference in the measured IC<sub>50</sub> for A2780 and A2780/AD cells for Mce<sub>6</sub> conjugated via non-degradable G and GG side chains. Conjugate **4** [P-(GFLG-Mce<sub>6</sub>)], however, was statistically more cytotoxic toward the A2780 than the A2780/AD cell line,  $p < 0.05$ , similar to values measured for free Mce<sub>6</sub> (Table 3). Free DOX and each HPMA copolymer-DOX conjugate, conjugates **6** [P-(GG-DOX)], **7** [P-(GG-DOX-mAb)], **8** [P-(GFLG-DOX)], and **9** [P-(GFLG-DOX-mAb)], were significantly more cytotoxic towards the A2780 versus the



A2780/AD cell line,  $p < 0.05$ . The cytotoxicity of HPMA copolymer/drug conjugates was increased by inclusion of a mAb targeting moiety for conjugates **3** [P-(GG-Mce<sub>6</sub>-mAb)], **7** [P-(GG-DOX-mAb)], and **9** [P-(GFLG-DOX-mAb)], versus conjugates **2** [P-(GG-Mce<sub>6</sub>)], **6** [P-(GG-DOX)], and **8** [P-(GFLG-DOX)], while conjugate **5** [P-(GFLG-Mce<sub>6</sub>-mAb)] showed a decreased cytotoxicity compared to conjugate **4** [P-(GFLG)-Mce<sub>6</sub>], for the A2780/AD cell line. In the A2780 cell line, the cytotoxicity of the non-targeted conjugates **4** [P-(GFLG)-Mce<sub>6</sub>], **6** [P-(GG-DOX)], and **8** [P-(GFLG-DOX)] were more cytotoxic than mAb targeted conjugates **5** [P-(GFLG-Mce<sub>6</sub>-mAb)], **7** [P-(GG-DOX-mAb)], and **9** [P-(GFLG-DOX-mAb)] (Table 3).

In contrast to similar IC<sub>50</sub> values for conjugate **3** [P-(GG-Mce<sub>6</sub>-mAb)] and conjugate **5** [P-(GFLG-Mce<sub>6</sub>-mAb)], conjugate **9** [P-(GFLG-DOX)-mAb], showed enhanced cytotoxicity toward A2780/AD cell line in comparison to conjugate **7** [P-(GG-DOX)-mAb] (Table 3). The similar IC<sub>50</sub> value for conjugates **3** [P-(GG-Mce<sub>6</sub>-mAb)] and **5** [P-(GFLG-Mce<sub>6</sub>-mAb)] may be due to primary localization of the targeted HPMA copolymer/drug conjugate to Pgp on the PM with limited and/or delayed internalization.<sup>[24]</sup> Reduced internalization as a result of PM localization or less internalization due to the 16h incubation time would decrease the amount of free Mce<sub>6</sub> liberated in the lysosomal compartment for A2780/AD cells. Conjugate **9** [P-(GFLG-DOX)-mAb], likely due to its primarily PM localization to Pgp, reduced the IC<sub>50</sub> dose measured for conjugate **8** [P-(GFLG-DOX)] by nearly an order of magnitude, almost to levels measured for free DOX (Table 3). The improved cytotoxicity is similar to results obtained with an internalized OV-TL16 antibody targeted HPMA copolymer/drug conjugates and the human ovarian cancer cell line OVCAR-3.<sup>[20]</sup> The increase in cytotoxicity of conjugate **9** [P-(GFLG-DOX)-mAb] may be similar to other non-internalized DOX conjugates, which demonstrate two to three orders of magnitude enhancement in DOX cytotoxicity over internalized free DOX.<sup>[48-50]</sup>

In all cases, UIC2 targeted HPMA copolymer/drug conjugates showed a higher IC<sub>50</sub> dose than non-targeted HPMA copolymer/drug conjugates for the A2780 cell line, demonstrating specificity (Table 3). The decreased cytotoxicity of UIC2 targeted HPMA copolymer/drug conjugates for A2780 cells and generally increased cytotoxicity in A2780/AD cells supports antigen specific enhancement of cytotoxicity. Similar studies in the literature utilizing targeted delivery systems indicated enhanced specificity to antigen expressing cells, although cytotoxicity can be induced by non-specific uptake of macromolecules.<sup>[51,52]</sup> The increased hydrophilicity of the mAb may also decrease interaction with cell membranes that do not express P-gp. Therefore, the amount of the UIC2 targeted HPMA copolymer/drug conjugate internalized versus non-targeted conjugates would decrease; the net result would be an increased IC<sub>50</sub> value, as seen in the A2780 cell line in this study.

### 3.4. Cell-Associated Mce<sub>6</sub>

The amount of free or HPMA copolymer/Mce<sub>6</sub> conjugates adsorbed to and inside the cell was determined following administration of the IC<sub>50</sub> dose (Table 3). The cell associated concentration increased with increasing IC<sub>50</sub> dose in a linear fashion, similar to trends demonstrated in the literature.<sup>[53]</sup> Calculation of the Pearson's correlation coefficient of the IC<sub>50</sub> dose versus cell associated Mce<sub>6</sub> was 0.96. This validates IC<sub>50</sub> values as a reliable

measure of the cytotoxicity of different forms of the drug for a given cell line, such as A2780/AD.

#### 4. Discussion

Multidrug resistance involves a number of mechanisms; overexpressed Pgp is one of the most common.<sup>[1]</sup> High-level expression of Pgp is found in normal tissues, generally characterized as barrier and excretory tissues.<sup>[54]</sup> Examples include: kidney, adrenal cortex, liver, colon, small bowel, brain, testis, and pancreas, with lower levels in a variety of tissues, including ovarian.<sup>[5,25,27]</sup> Expression of Pgp explains the MDR prevalence in tissues prior to treatment and induction of MDR in ovarian cancer following anti-cancer drug exposure. Alternative strategies in development to target Pgp include inhibitors,<sup>[3,25,26,55]</sup> mAb that target and partially reverse Pgp efflux,<sup>[32,33,56,57]</sup> and utilization of anti-Pgp mAb effector function to trigger antibody dependent cellular toxicity or complement dependent cytotoxicity.<sup>[58,59]</sup> To date, no clear strategy has demonstrated sufficient effect to overcome MDR.

Another strategy is bypassing Pgp efflux using HPMA copolymer/drug conjugates, which passively increase the uptake of macromolecules into tumors by the EPR effect.<sup>[11,13,14]</sup> HPMA copolymer/DOX conjugates, as well as other HPMA copolymer/drug conjugates, have been utilized in a number of clinical trials to test this strategy.<sup>[60,61]</sup> Conjugation of anti-cancer drugs to degradable GFLG side chains was designed to allow the release of the drug once the HPMA copolymer/drug conjugates reaches the lysosomal compartment.<sup>[62]</sup> A lysosomotropic drug delivery system was demonstrated using OV-TL16 antibody targeted HPMA copolymer/DOX conjugates directed against the OA3 antigen of OVCAR-3 cells.<sup>[20]</sup> Conjugated DOX localized in the lysosomal compartment in OVCAR-3 cells for OV-TL16 antibody targeted HPMA copolymer/DOX conjugates containing non-degradable side chains, and for released DOX in the nucleus for conjugates containing degradable side chains.<sup>[20]</sup> Additional studies highlighted differing localization of HPMA copolymer/drug conjugates dependent on the mechanism and the target (targeted conjugates).<sup>[19,23,34]</sup>

Localization studies with UIC2 targeted conjugate **11** [P-(AP-FITC)-mAb] exhibited primarily PM localization (Figure 3D), similar to studies examining Pgp function and localization noted in the literature.<sup>[8,24–28]</sup> Limited intracellular localization within early endosomes and lysosomes does occur for Pgp, and may occur for HPMA copolymer/drug conjugates targeted with the UIC2 antibody.<sup>[8,24,28]</sup> While Pgp is primarily localized at the PM, a number of studies have identified compounds that alter Pgp localization either by interference with protein/protein complexes or inhibitors of energy dependent pathways which alter the localization and internalization of Pgp.<sup>[25–27,54,63–65]</sup> Images of conjugate **11** [P-(AP-FITC)-mAb] incubated with A2780/AD cells does exhibit limited internalization within the cells, and based on trafficking studies of Pgp in the literature, it is within early endosomes or lysosomes, and not within recycling endosomes.<sup>[6,64]</sup> If alteration of Pgp trafficking had occurred, a more intense fluorescence near the perinuclear region, as found for conjugate **10** [P-(AP-FITC)], would be evident.<sup>[20,40]</sup> Localization of HPMA copolymer conjugates was studied using FITC labeled conjugates, rather than DOX, as alterations in DOX fluorescence occur due to DNA intercalation, effects of the cell medium, whether the

cells are sensitive or resistant to anti-cancer agents and the presence of DOX metabolites.<sup>[66]</sup> Recently a method has been developed that allows discrimination between DOX and one of the key metabolites that distributes differently in sensitive and drug-resistant cell lines.<sup>[67]</sup> Discrimination between DOX and DOX metabolites may allow a clearer distinction in intracellular accumulation of anti-Pgp HPMA copolymer/DOX conjugates and aid in our understanding of methods to overcome MDR.

As noted above, the alteration of Pgp expression at the PM is a potential target for circumvention of MDR, but this was not noted for anti-Pgp-targeted HPMA copolymers (without drug). UIC2 targeted HPMA copolymer/drug conjugates, therefore, offered an opportunity to specifically target MDR cells over-expressing Pgp and demonstrate their specificity and efficacy when primarily localized to the PM. Additional studies of anti-Pgp targeted HPMA copolymer/drug conjugates are warranted to investigate if the inclusion of a drug moiety alters the localization of Pgp.

Many anti-cancer agents require localization within the cell for activity, which may somewhat limit the use of anti-Pgp mAb as a means to target MDR cell lines. The photosensitizer Mce<sub>6</sub> and the anti-neoplastic agent DOX, which both exhibit membrane activity, were selected due to their ability to be toxic by mechanisms that do not require cell entry. Targeted HPMA copolymer/drug conjugates (Mce<sub>6</sub> or DOX) exhibited the ability to induce cell death through photodynamic therapy (PDT) using Mce<sub>6</sub>,<sup>[68,69]</sup> and presumably by membrane activity of the anti-cancer agent DOX.<sup>[48–50,70]</sup> Enhanced cytotoxicity of PM localized UIC2 targeted HPMA copolymer/drug conjugates towards A2780/AD cells was demonstrated for three of the four conjugates tested (Table 3). Conjugate 3 [P-(GG-Mce<sub>6</sub>)-mAb], exhibited a threefold higher cytotoxicity than conjugate 2 [P-(GG-Mce<sub>6</sub>)]. Conjugate 7 [P-(GG-DOX)-mAb] and conjugate 9 [P-(GFLG-DOX)-mAb] were four- and eightfold lower IC<sub>50</sub> values than conjugates 6 [P-(GG-DOX)] and 8 [P-(GFLG-DOX)], respectively. As noted for conjugate 4 [P-(GFLG)-Mce<sub>6</sub>] versus conjugate 5 [P-(GFLG-Mce<sub>6</sub>)-mAb], targeting Pgp with HPMA copolymer/drug conjugates containing Mce<sub>6</sub> reduced the cytotoxicity against the A2780/AD cell line in vitro. The exact mechanism would require further study, but may be related to the diminished internalization of Pgp from the PM. Reduced cytotoxicity of conjugate 5 [P-(GFLG-Mce<sub>6</sub>)-mAb] may be partially explained by the reduced production of singlet oxygen of Mce<sub>6</sub> bound to conjugate 5 [P-(GFLG-Mce<sub>6</sub>)-mAb] as a result of localization at the PM.<sup>[71]</sup>

Plasma membrane localization demonstrated photo-activation of Mce<sub>6</sub> conjugated to antibody targeted macromolecules, generation of singlet oxygen, and creation of oxygenated products leading to single point rupture of the cell.<sup>[69]</sup> DOX typically known to be cytotoxic via intercalation with DNA and stabilization of the cleavable complex between topoisomerase and DNA,<sup>[72]</sup> has been shown to possess membrane activity at the PM when immobilized to non-internalized drug delivery systems,<sup>[50,70]</sup> and HPMA copolymer/drug conjugates have demonstrated cytotoxicity as a result of damage to cellular membranes.<sup>[19]</sup>

Cell death caused by PM localized photosensitizers, i.e., UIC2 targeted HPMA copolymer-Mce<sub>6</sub> conjugates, occurs by lipid peroxidation and PM protein oxidation. Non-internalized DOX conjugates, similar to UIC2 targeted HPMA copolymer/DOX conjugates, destabilize

the PM and induce cell death.<sup>[48–50]</sup> Targeting of Pgp and localization to the PM may enhance anti-cancer treatments for MDR cell lines by bypassing resistant mechanisms which occur following diffusion or endocytosis of anti-cancer agents into the cell, i.e., reduced drug accumulation, altered localization, increased detoxification, and enhanced DNA repair.

The increased cytotoxicity of DOX conjugate **9** [P-(GFLG-DOX-mAb)] versus **8** [P-(GFLG-DOX)] in contrast to the decreased cytotoxicity of Mce<sub>6</sub> conjugate **5** [P-(GFLG-Mce<sub>6</sub>)-mAb] versus **4** [P-(GFLG)-Mce<sub>6</sub>] may be due to the membrane cytotoxicity of immobilized DOX, which has been shown to be two to three orders of magnitude more cytotoxic than internalized free DOX.<sup>[48–50]</sup> Another potentially contributing factor is the difference in the incubation period for DOX conjugates versus their Mce<sub>6</sub> counterparts. The study was designed to compare drug effects for the same period of drug activity (72 h), following exposure to DOX conjugates or activation of Mce<sub>6</sub> conjugates by irradiation. Further study is required to identify if the length of the incubation period for anti-Pgp HPMA copolymer/Mce<sub>6</sub> conjugates, i.e., >16 h, would alter its cytotoxicity versus the non-targeted conjugate.

Cytotoxicity without nuclear accumulation of non-internalized macromolecule/DOX conjugates was demonstrated with transferrin/DOX conjugates, which exhibited membrane activity, similar to other immobilized DOX models.<sup>[50,73–75]</sup> The insertion depth and membrane destabilization of non-internalized DOX conjugates are dependent on a number of factors involving the chemical structure of anthracyclines.<sup>[76,77]</sup> The chemical structure of side chains of HPMA copolymer/DOX conjugates, the density of Pgp, and the number of DOX per conjugate may also influence the ability of DOX to destabilize the membrane.<sup>[19,34]</sup> The decreased IC<sub>50</sub> dose of conjugate **9** [P-(GFLG-DOX-mAb)] versus conjugate **7** [P-(GG-DOX-mAb)] for A2780/AD cells could reflect differences in the oligopeptide side chains used to link DOX to the HPMA copolymer backbone, and result in variation in the ability to disrupt the membrane.<sup>[19,34]</sup> One may hypothesize that the cell membrane may serve to solubilize the aggregates, and at the same time destabilize the phospholipid bilayer due to an increase in the local concentration of DOX.<sup>[19,34,50,78]</sup>

The effect may also be related to enhanced inhibition of Pgp as noted for co-incubation of UIC2 in the presence of Pgp substrates.<sup>[33]</sup> Incubation in vitro of Pgp expressing cells in the presence of UIC2 and Pgp substrates enhanced both the amount of Pgp available for UIC2 binding and the inhibition of Pgp as a result of UIC2 binding. The enhanced cytotoxicity of anti-Pgp-targeted HPMA copolymer/DOX conjugates may involve a similar mechanism, since DOX is a substrate of Pgp, while Mce<sub>6</sub> is not. The intercalation of DOX into the PM may increase the number of available Pgp available for UIC2 recognition; further increasing the cytotoxic effect. In contrast to UIC2 targeted conjugate **7** [P-(GG-DOX)-mAb], anti-Thy 1.2 or anti-Lak antibodies targeted to the lymphatic system conjugated to HPMA copolymer/DOX conjugates with GG spacers exhibited no inhibition of antibody production, while similar conjugates containing GFLG spacers were more efficient than free DOX in vivo.<sup>[79]</sup> The enhanced cytotoxicity of conjugate **7** [P-(GG-DOX)-mAb] in comparison to anti-Thy 1.2 or anti-Lak-targeted HPMA copolymer/DOX conjugates with GG spacers may be due to an altered mechanism which occurs due to its localization to the PM.<sup>[79]</sup>

In addition to the supporting evidence of specificity noted above, the efficacy and specificity of targeted HPMA copolymer/Mce<sub>6</sub> conjugates localized to the PM was confirmed by comparing the cytotoxicity of targeted and non-targeted HPMA copolymer/drug conjugates. Differences in non-antigen expressing A2780 cells and antigen (Pgp) expressing A2780/AD cell lines, similar to methods cited in the literature, demonstrate the enhanced specificity of antibody targeting toward antigen expressing cell lines.<sup>[51,80]</sup>

UIC2-targeted HPMA copolymer/drug conjugates exhibit the ability to increase cytotoxicity towards MDR carcinoma following binding to Pgp localized at the PM. Selection of anti-cancer agents that exhibit cytotoxicity at the PM was essential. The ability to induce cell death while conjugated to a macromolecule was demonstrated for a photo sensitizer, Mce<sub>6</sub>, and the antineoplastic agent DOX. The hypothesized mechanism for action is different for each compound, lipid and PM protein peroxidation for Mce<sub>6</sub> and PM destabilization for DOX, but the concentration dependent cytotoxicity against A2780/AD cells was similar. Recent research has highlighted new potential methods to specifically target Pgp.<sup>[25–27,54,63–65]</sup> A deeper understanding of the intracellular trafficking and the pathways involved in Pgp expression and function will continue to expand the potential targets to mitigate or eliminate MDR due to Pgp overexpression.

## Acknowledgements

The research was supported in part by NIH grant CA51578 from the National Cancer Institute. We thank Dr. Pavla Kopecková for valuable discussions.

## Nomenclature

<b>AP</b>	1-amino-2-propanol
<b>BCA</b>	bicinchoninic acid
<b>BSA</b>	bovine serum albumin
<b>DOX</b>	doxorubicin
<b>DPBS</b>	Dulbecco's phosphate-buffered saline
<b>EPR</b>	enhanced permeability and retention
<b>FITC</b>	fluorescein isothiocyanate
<b>G</b>	glycine
<b>GG</b>	glycylglycine
<b>GFLG</b>	glycylphenylalanylleucylglycine
<b>HBSS</b>	Hank's balanced salt solution
<b>HPMA</b>	<i>N</i> -(2-hydroxypropyl)methacrylamide
<b>IC<sub>50</sub></b>	inhibitory concentration at which 50% of cell growth is inhibited relative to control cells
<b>MA</b>	methacryloyl

<b>mAb</b>	monoclonal antibody
<b>Mce<sub>6</sub></b>	mesochlorin e <sub>6</sub> mono ( <i>N</i> -2-amino-ethylamide)
<b>MDR</b>	multidrug resistance
<b>MTT</b>	3-(4,5-dimethylthiazol-2-yl)-2,5-diphenyltetrazolium bromide
<b>ONp</b>	<i>p</i> -nitrophenyl ester
<b>P</b>	HPMA copolymer backbone
<b>P-(G-Mce<sub>6</sub>)</b>	HPMA copolymer/Mce <sub>6</sub> conjugate containing G spacer
<b>P-(GG-Mce<sub>6</sub>)</b>	HPMA copolymer/Mce <sub>6</sub> conjugate containing GG spacer
<b>P-(GFLG-Mce<sub>6</sub>)</b>	HPMA copolymer/Mce <sub>6</sub> conjugate containing GFLG spacer
<b>P-(GG-Mce<sub>6</sub>)-mAb</b>	UIC2-targeted HPMA copolymer-Mce <sub>6</sub> conjugate containing GG spacer
<b>P-(GFLG-Mce<sub>6</sub>)-mAb</b>	UIC2-targeted HPMA copolymer-Mce <sub>6</sub> conjugate containing GFLG spacer
<b>P-(GG-DOX)</b>	HPMA copolymer/DOX conjugate containing GG spacer
<b>P-(GFLG-DOX)</b>	HPMA copolymer/DOX conjugate containing GFLG spacer
<b>P-(GG-DOX)-mAb</b>	UIC2-targeted HPMA copolymer-DOX conjugate containing GG spacer
<b>P-(GFLG-DOX)-mAb</b>	UIC2-targeted HPMA copolymer-DOX conjugate containing GFLG spacer
<b>P-(AP-FITC)</b>	HPMA copolymer conjugate containing fluorescein
<b>P-(AP-FITC)-mAb</b>	UIC2-targeted HPMA copolymer conjugates containing fluorescein and a G spacer
<b>PDT</b>	photodynamic therapy
<b>Pgp</b>	P-glycoprotein
<b>PM</b>	plasma membrane
<b>RT</b>	room temperature
<b>SDS-PAGE</b>	sodium dodecylsulfate polyacrylamide gel electrophoresis
<b>SMCC</b>	4-(maleimidomethyl)cyclohexane-carboxylic acid <i>N</i> -hydroxysuccinimide ester

## References

1. Aller SG, Yu J, Ward A, Weng Y, Chittaboina S, Zhuo R, Harrell PM, Trinh YT, Zhang Q, Urbatsch IL, Chang G. *Science*. 2009; 323:1718. [PubMed: 19325113]
2. Litman T, Druley TE, Stein WD, Bates SE. *Cell. Mol. Life Sci*. 2001; 58:931. [PubMed: 11497241]
3. Scala S, Akhmed N, Rao US, Paull K, Lan LB, Dickstein B, Lee JS, Elgemeie GH, Stein WD, Bates SE. *Mol. Pharmacol*. 1997; 51:1024. [PubMed: 9187269]



4. Goda K, Bacso Z, Szabo G. *Curr. Cancer Drug Targets*. 2009; 9:281. [PubMed: 19442049]
5. Jigorel E, Le Vee M, Boursier-Neyret C, Parmentier Y, Fardel O. *Drug Metab. Dispos.* 2006; 34:1756. [PubMed: 16837569]
6. Willingham MC, Richert ND, Cornwell MM, Tsuruo T, Hamada H, Gottesman MM, Pastan IH. *J. Histochem. Cytochem.* 1987; 35:1451. [PubMed: 2890686]
7. Hennessy M, Spiers JP. *Pharmacol. Res.* 2007; 55:1. [PubMed: 17095241]
8. Shapiro AB, Fox K, Lee P, Yang YD, Ling V. *Int. J. Cancer.* 1998; 76:857. [PubMed: 9626353]
9. Arancia G, Molinari A, Calcabrini A, Meschini S, Cianfriglia M. *Ital. J. Anat. Embryol.* 2001; 106:59. [PubMed: 11729998]
10. Shiah JG, Dvo ak M, Kope kov P, Sun Y, Peterson CM, Kope ek J. *Eur. J. Cancer.* 2001; 37:131. [PubMed: 11165140]
11. Kope ek J, Kope kov P. *Adv. Drug Deliv. Rev.* 2010; 62:122. [PubMed: 19919846]
12. Malugin A, Kope kov P, Kope ek J. *Mol. Pharm.* 2006; 3:351. [PubMed: 16749867]
13. Maeda H, Seymour LW, Miyamoto Y. *Bioconjugate Chem.* 1992; 3:351.
14. Noguchi Y, Wu J, Duncan R, Strohal J, Ulbrich K, Akaike T, Maeda H. *Jpn. J. Cancer Res.* 1998; 89:307. [PubMed: 9600125]
15. Minko T, Kope kov P, Pozharov V, Kope ek J. *J. Controlled Release.* 1998; 54:223.
16. Št'astn M, Strohal J, Plocov D, Ulbrich K, hov B. *Eur. J. Cancer.* 1999; 35:459. [PubMed: 10448300]
17. Malugin A, Kope kov P, Kope ek J. *J. Controlled Release.* 2007; 124:6.
18. Liu J, Kope kov P, Buhler P, Wolf P, Pan H, Bauer H, Elsasser-Beile U, Kope ek J. *Mol. Pharm.* 2009; 6:959. [PubMed: 19344119]
19. Hovorka O, Etrych T, Šubr V, Strohal J, Ulbrich K. B. hov J. *Drug Target.* 2006; 14:391. [PubMed: 17092839]
20. Omelyanenko V, Gentry C, Kope kov P, Kope ek J. *Int. J. Cancer.* 1998; 75:600. [PubMed: 9466663]
21. hov B, Jelinkov M, Strohal J, Šubr V, Plocov D, Hovork O, Novk M, Plundrov D, Germano Y, Ulbrich K. *J. Controlled Release.* 2000; 64:241.
22. Jelinkov M, Strohal J, Plocov D, Šubr V, Št'astn M, Ulbrich K, hov B. *J. Controlled Release.* 1998; 52:253.
23. Ulbrich K, Etrych T, Chytil P, Jelinkov M, hov B. *J. Drug Target.* 2004; 12:477. [PubMed: 15621674]
24. Fu D, Roufogalis BD. *Am. J. Physiol. Cell Physiol.* 2006; 292:C1543. [PubMed: 17122416]
25. Hawkins BT, Sykes DB, Miller DS. *J. Neurosci.* 2010; 30:1417. [PubMed: 20107068]
26. Slomiany MG, Dai L, Bomar PA, Knackstedt TJ, Kranc DA, Tolliver L, Maria BL, Toole BP. *Cancer Res.* 2009; 69:4992. [PubMed: 19470767]
27. Ortiz DF, Moseley J, Calderon G, Swift AL, Li S, Arias IM. *J. Biol. Chem.* 2004; 279:32761. [PubMed: 15159385]
28. Kim H, Barroso M, Samanta R, Greenberger L, Sztul E. *Am. J. Physiol.* 1997; 273:C687. [PubMed: 9277367]
29. Vrouenraets MB, Visser GW, Stewart FA, Stigter M, Oppelaar H, Postmus PE, Snow GB, van Dongen GA. *Cancer Res.* 1999; 59:1505. [PubMed: 10197621]
30. Lehne G, De Angelis P, Clausen OP, Egeland T, Tsuruo T, Rugstad HE. *Cytometry.* 1995; 20:228. [PubMed: 7587708]
31. Schinkel AH, Arceci RJ, Smit JJ, Wagenaar E, Baas F, Dolle M, Tsuruo T, Mechetner EB, Roninson IB, Borst P. *Int. J. Cancer.* 1993; 55:478. [PubMed: 8104165]
32. Krasznai ZT, Toth A, Mikecz P, Fodor Z, Szabo G, Galuska L, Hernadi Z, Goda K. *Eur. J. Pharm. Sci.* 2010; 41:665. [PubMed: 20869436]
33. Goda K, Fenyvesi F, Bacso Z, Nagy H, Marian T, Megyeri A, Krasznai Z, Juhasz I, Vecsernyes M, Szabo G Jr. *J. Pharmacol. Exp. Ther.* 2007; 320:81. [PubMed: 17050779]
34. hov B, Strohal J, Hovorka O, Šubr V, Etrych T, Chytil P, Pola R, Plocov D, Bou ek J, Ulbrich K. *J. Controlled Release.* 2008; 127:110.

35. Louie KG, Behrens BC, Kinsella TJ, Hamilton TC, Grotzinger KR, McKoy WM, Winker MA, Ozols RF. *Cancer Res.* 1985; 45:2110. [PubMed: 3986765]
36. Fowers KD, Callahan J, Byron P, Kopeček J. *J. Drug Target.* 2001; 9:281. [PubMed: 11697031]
37. Kopeček J, Bažilová H. *Eur. Polym. J.* 1973; 9:7.
38. Rejmanová P, Labský J, Kopeček J. *Makromol. Chem.* 1977; 178:2159.
39. Šňohová B, Bilej M, Vrtiška V, Ulbrich K, Strohalm J, Kopeček J, Duncan R. *Biomaterials.* 1989; 10:335. [PubMed: 2765631]
40. Omelyanenko V, Kopečková P, Gentry C, Kopeček J. *J. Controlled Release.* 1998; 53:25.
41. Omelyanenko V, Kopečková P, Gentry C, Shiah JG, Kopeček J. *J. Drug Target.* 1996; 3:357. [PubMed: 8866655]
42. Hansen MB, Nielsen SE, Berg K. *J. Immunol. Methods.* 1989; 119:203. [PubMed: 2470825]
43. Johnson, FH.; Eyring, H.; Stover, BJ. *The Theory of Rate Processes in Biology and Medicine.* New York: John Wiley & Sons; 1974.
44. Opreško LK, Chang CP, Will BH, Burke PM, Gill GN, Wiley HS. *J. Biol. Chem.* 1995; 270:4325. [PubMed: 7876194]
45. Mechetner EB, Roninson IB. *Proc. Natl. Acad. Sci. USA.* 1992; 89:5824. [PubMed: 1352877]
46. Rejmanová P, Kopeček J, Duncan R, Lloyd JB. *Biomaterials.* 1985; 6:45. [PubMed: 3971018]
47. Duncan R, Seymour LC, Scarlett L, Lloyd JB, Rejmanová P, Kopeček J. *Biochim. Biophys. Acta.* 1986; 880:62. [PubMed: 3942780]
48. Bertelli R, Ginevri F, Gusmano R, Ghiggeri GM. *In vitro Cell. Dev. Biol.* 1991; 27A:799. [PubMed: 1960147]
49. Jeannesson P, Trentesaux C, Gerard B, Jardillier JC, Ross KL, Tokes ZA. *Cancer Res.* 1990; 50:1231. [PubMed: 2297771]
50. Tritton TR. *Pharmacol. Ther.* 1991; 49:293. [PubMed: 2052627]
51. Hu LK, Hasan T, Gragoudas ES, Young LH. *Exp. Eye Res.* 1995; 61:385. [PubMed: 8549679]
52. Morgan J, Gray AG, Huehns ER. *Br. J. Cancer.* 1989; 59:366. [PubMed: 2930700]
53. Schuurhuis GJ, van Heijningen TH, Cervantes A, Pinedo HM, de Lange JH, Keizer HG, Broxterman HJ, Baak JP, Lankelma J. *Br. J. Cancer.* 1993; 68:898. [PubMed: 8105865]
54. Miller DS, Bauer B, Hartz AM. *Pharmacol. Rev.* 2008; 60:196. [PubMed: 18560012]
55. Shukla S, Robey RW, Bates SE, Ambudkar SV. *Drug Metab. Dispos.* 2009; 37:359. [PubMed: 18971320]
56. Pearson JW, Fogler WE, Volker K, Usui N, Goldenberg SK, Gruys E, Riggs CW, Komschlies K, Wiltrott RH, Tsuruo T, Pastan I, Gottesman MM, Longo DL. *J. Natl. Cancer Inst.* 1991; 83:1386. [PubMed: 1681110]
57. Raghu G, Park SW, Roninson IB, Mechetner EB. *Exp. Hematol.* 1996; 24:1258. [PubMed: 8765502]
58. Iwahashi T, Okochi E, Ariyoshi K, Watabe H, Amann E, Mori S, Tsuruo T, Ono K. *Cancer Res.* 1993; 53:5475. [PubMed: 8106147]
59. Sutherland MK, Yu C, Lewis TS, Miyamoto JB, Morris-Tilden CA, Jonas M, Sutherland J, Nesterova A, Gerber HP, Sievers EL, Grewal IS, Law CL. *MAbs.* 2009; 1:481. [PubMed: 20065652]
60. Duncan R, Vicent MJ. *Adv. Drug Deliv. Rev.* 2010; 62:272. [PubMed: 20005271]
61. Vasey PA, Kaye SB, Morrison R, Twelves C, Wilson P, Duncan R, Thomson AH, Murray LS, Hilditch TE, Murray T, Burtles S, Fraier D, Frigerio E, Cassidy J. *Clin. Cancer Res.* 1999; 5:83. [PubMed: 9918206]
62. Rejmanová P, Pohl J, Baudyš M, Kostka V, Kopeček J. *Makromol. Chem.* 1983; 184:2009.
63. Ferrandiz-Huertas C, Fernandez-Carvajal A, Ferrer-Montiel A. *Int. J. Cancer.* 2011; 128:192. [PubMed: 20209493]
64. Fu D, van Dam EM, Brymora A, Duggin IG, Robinson PJ, Roufogalis BD. *Biochim. Biophys. Acta.* 2007; 1773:1062. [PubMed: 17524504]
65. Porcelli L, Lemos C, Peters GJ, Paradiso A, Azzariti A. *Curr. Top. Med. Chem.* 2009; 9:197. [PubMed: 19200005]

66. Fiallo M, Laigle A, Borrel M, Garnier-Suillerot A. *Biochem. Pharmacol.* 1993; 45:659. [PubMed: 8095138]
67. Hovorka O, Šubr V, Vtvička D, Kovář J, Strohalm L, Strohalm M, Benda A, Hof M, Ulbrich K, Říhová B. *Eur. J. Pharm. Biopharm.* 2010; 76:514. [PubMed: 20638475]
68. Girotti AW, Deziel MR. *Adv. Exp. Med. Biol.* 1983; 160:213. [PubMed: 6837353]
69. Thorpe WP, Toner M, Ezzell RM, Tompkins RG, Yarmush ML. *Biophys. J.* 1995; 68:2198. [PubMed: 7612864]
70. Grunicke H, Hofmann J. *Pharmacol. Ther.* 1992; 55:1. [PubMed: 1287673]
71. Krinick NL, Sun Y, Joyner D, Spikes JD, Straight RC, Kopeček J. *J. Biomater. Sci. Polym. Ed.* 1994; 5:303. [PubMed: 8025029]
72. Tewey KM, Rowe TC, Yang L, Halligan BD, Liu LF. *Science.* 1984; 226:466. [PubMed: 6093249]
73. Barabas K, Sizensky JA, Faulk WP. *J. Biol. Chem.* 1992; 267:9437. [PubMed: 1577771]
74. Goormaghtigh E, Chatelain P, Caspers J, Ruyschaert JM. *Biochem. Pharmacol.* 1980; 29:3003. [PubMed: 7458950]
75. Henry N, Fantine EO, Bolard J, Garnier-Suillerot A. *Biochemistry.* 1985; 24:7085. [PubMed: 4084563]
76. Burke TG, Tritton TR. *Biochemistry.* 1985; 24:5972. [PubMed: 3866609]
77. Rapoport N, Pitina LJ. *Pharm. Sci.* 1998; 87:321.
78. Keizer HG, Pinedo HM, Schuurhuis GJ, Joenje H. *Pharmacol. Ther.* 1990; 47:219. [PubMed: 2203071]
79. Říhová B, Kopečková P, Strohalm J, Rossmann P, Vtvička V, Kopeček J. *Clin. Immunol. Immunopathol.* 1988; 46:100. [PubMed: 2891460]
80. Hamblin MR, Miller JL, Hasan T. *Cancer Res.* 1996; 56:5205. [PubMed: 8912858]

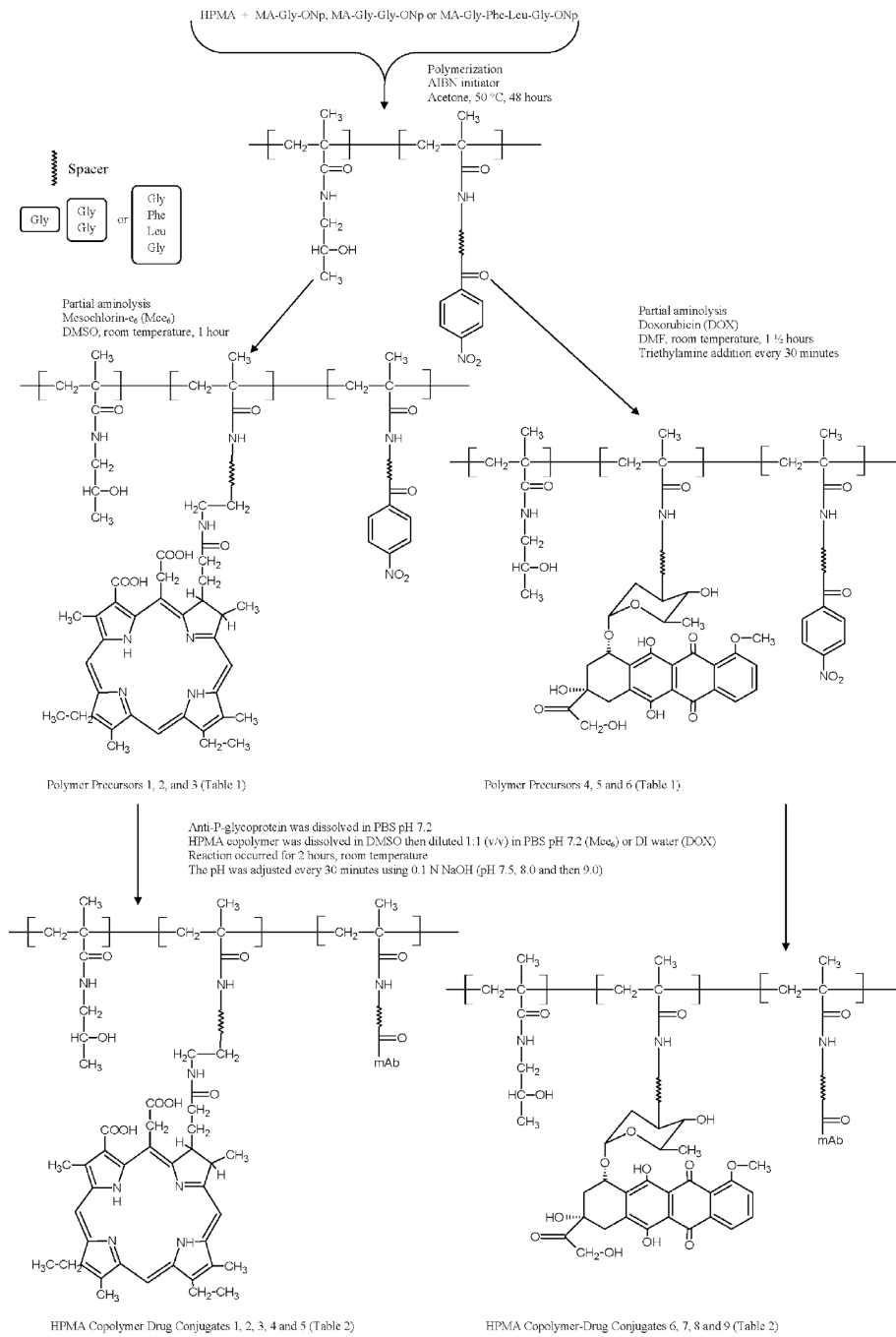


**Figure 1.**  
Chemical structure of HPMA copolymer/drug conjugates.

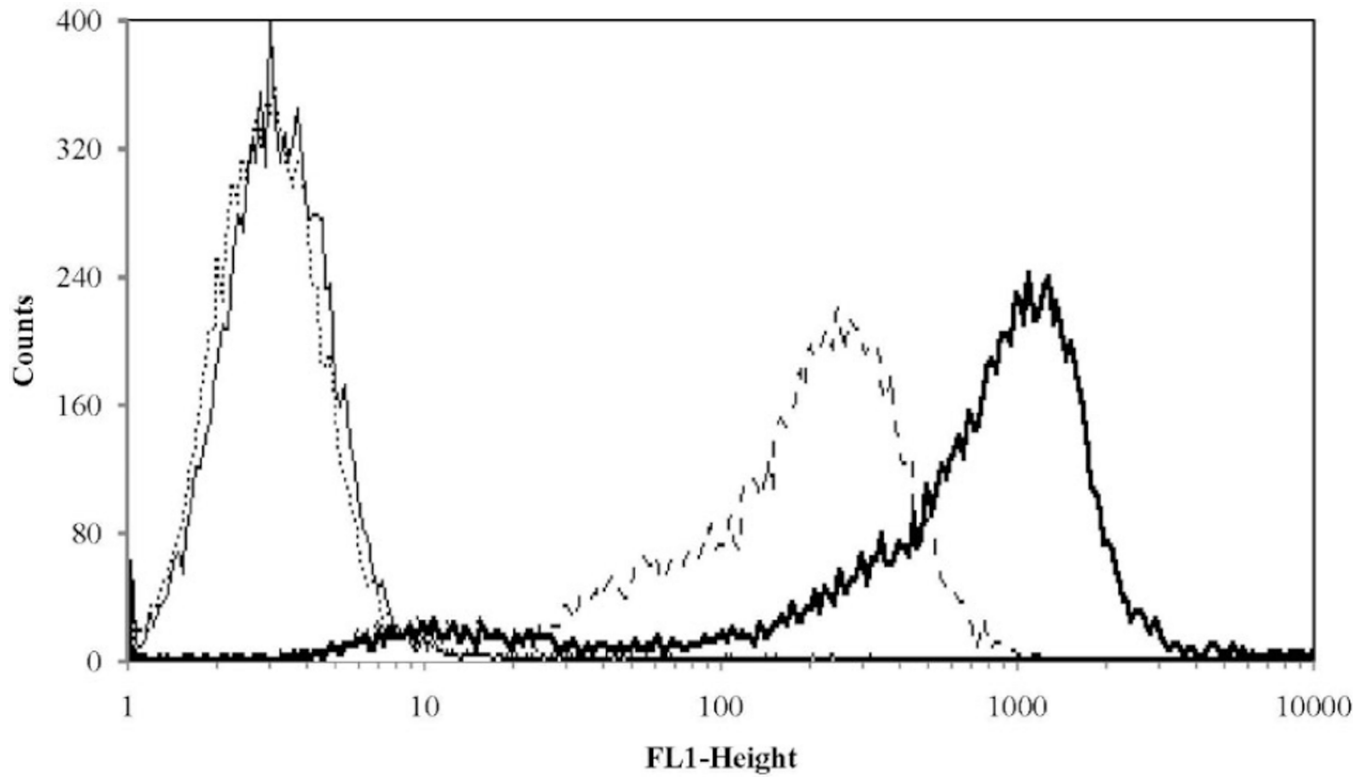


**Figure 2.**

Flow cytometry analysis of P-glycoprotein expression on the human ovarian cancer cell line A2780/AD: (—) A2780 control cells; (···) A2780 control cells exposed to fluorescein labeled anti-mouse IgG; (---) A2780/AD cells exposed to P-(AP-FITC)-mAb; and (—) A2780/AD cells exposed to UIC2 mAb followed by fluorescein labeled anti-mouse IgG. FL1-Height is the relative intensity of fluorescein.

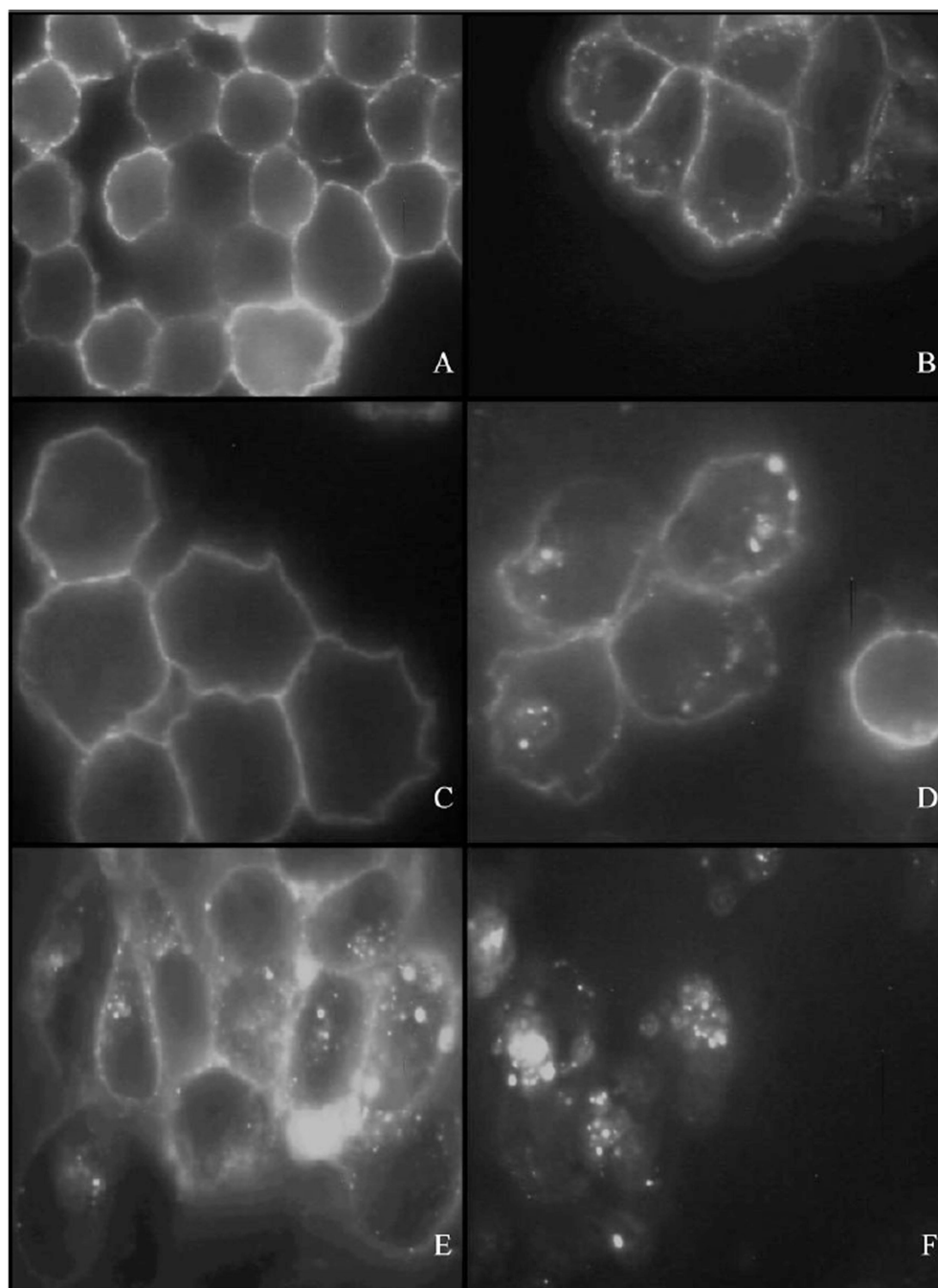


**Figure 3.** Fluorescent microscopy images of A2780/AD cells incubated with UIC2 antibodies followed by fluorescein labeled anti-mouse IgG for 16 h at 4 (A) or 37°C (B), with conjugate **11** [P-(AP-FITC)-mAb] for 16h at 4 (C) or 37°C (D), and with conjugate **11** [P-(AP-FITC)-mAb] for 48h at 37°C (E) and conjugate **10** [P-(AP-FITC)] for 16 h at 37°C (F).



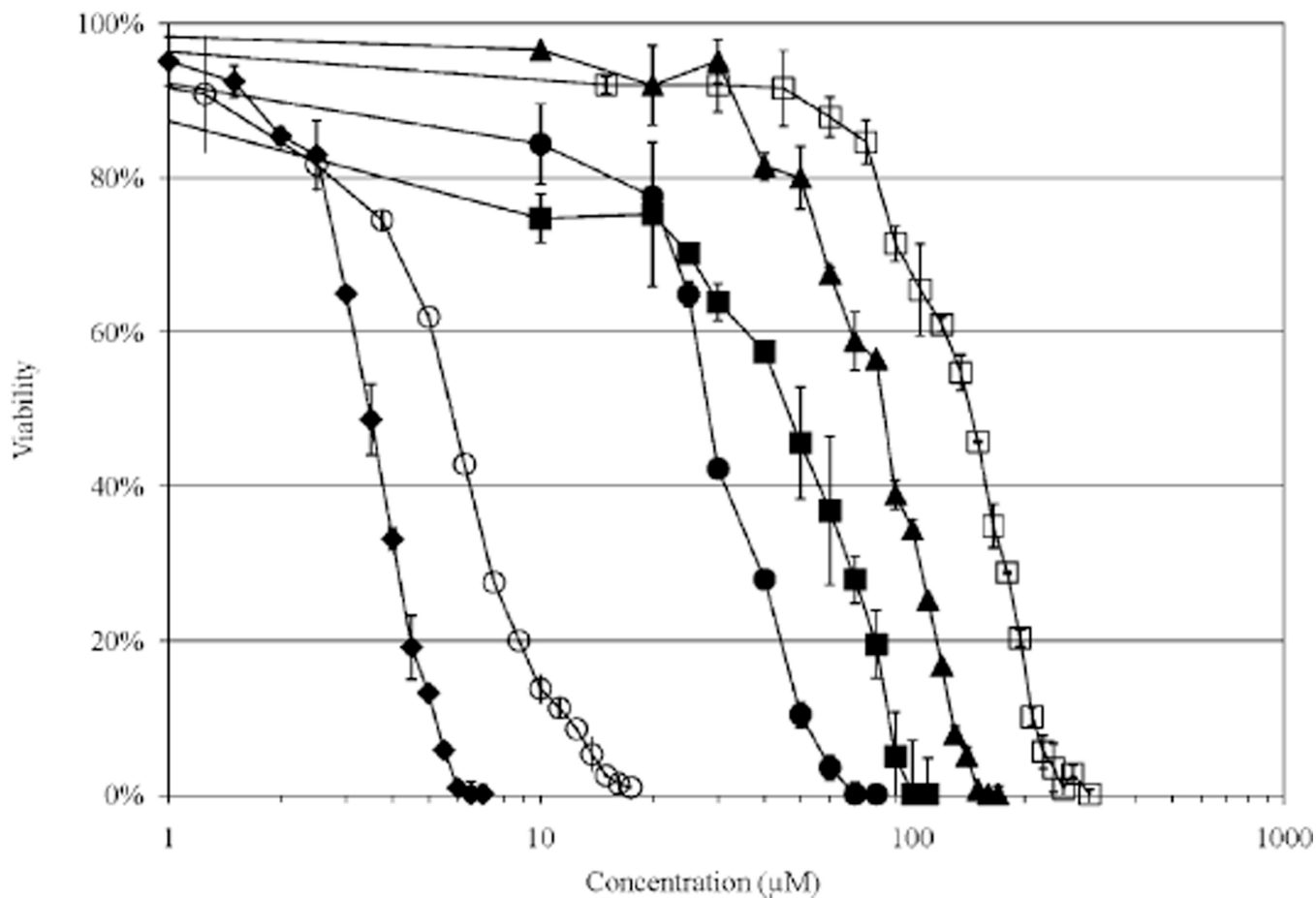


**Figure 4.** Viability of A2780/AD cells as a function of Mce<sub>6</sub> concentration. The cytotoxicity of targeted and non-targeted HPMA copolymer/drug conjugates was determined using a modified MTT assay. Typical dose-response curves are shown for free Mce<sub>6</sub> (-◆-); P-(G-Mce<sub>6</sub>) (-▲-); P-(GG-Mce<sub>6</sub>) (-□-); P-(GFLG-Mce<sub>6</sub>) (-○-); P-(GG-Mce<sub>6</sub>)-mAb (-■-); and P-(GFLG-Mce<sub>6</sub>)-mAb (-●-).

**Table 1**

Characterization of HPMA copolymer/drug conjugates containing residual ONp groups.

Polymer precursor	Structure	Approximate molecular ratio		
		ONp	Polymer	Drug
1	P-(G-Mce <sub>6</sub> )-ONp	4.1	1	4.3
2	P-(GG-Mce <sub>6</sub> )-ONp	n.d.	1	8.4
3	P-(GFLG-Mce <sub>6</sub> )-ONp	3.5	1	8.0
4	P-(GG-DOX)-ONp	6.8	1	2.8
5	P-(GFLG-DOX)-ONp	8.5	1	4.1
6	P-(AP-FITC)-ONp	4.7	1	3.3

Author Manuscript

Author Manuscript

Author Manuscript

Author Manuscript

Table 2

Characterization of HPMA copolymer/drug conjugates.

Number	Structure	Composition <sup>a)</sup>				$M_w^{b)}$ [kDa]		
		[wt%]		mol. ratio				
		Protein	Polymer	Drug	Protein	Polymer	Drug	
1	P-(G-Mce <sub>6</sub> )	-	84.9	15.0	-	1	4	19
2	P-(GG-Mce <sub>6</sub> )	-	83.9	16.1	-	1	6	25
3	P-(GG-Mce <sub>6</sub> )-mAb	68.9	26.6	4.6	1	2.3	12	208
4	P-(GFLG-Mce <sub>6</sub> )	-	79.2	20.8	-	1	7.4	23
5	P-(GFLG-Mce <sub>6</sub> )-mAb	52.8	37.3	9.9	1	4.6	34	256
6	P-(GG-DOX)	-	88.5	11.5	-	1	3	n.d.
7	P-(GG-DOX)-mAb	63.4	32.8	3.8	1	3	8.2	n.d.
8	P-(GFLG-DOX)	-	87.1	12.9	-	1	3.9	23
9	P-(GFLG-DOX)-mAb	74.7	25.3	3.3	1	2.2	6.7	200
10	P-(AP-FITC)	-	96.8	3.2	-	1	1.3	19
11	P-(AP-FITC)-mAb	70.9	28.2	0.9	1	3.2	3.6	211

<sup>a)</sup> Polymer content was based on Mce<sub>6</sub>, DOX, or fluorescein absorbance using  $\epsilon_{394\text{nm}} = 1.58 \times 10^5 \text{ L} \cdot \text{mol}^{-1} \cdot \text{cm}^{-1}$  in MeOH,  $\epsilon_{490\text{nm}} = 1.1 \times 10^4 \text{ L} \cdot \text{mol}^{-1} \cdot \text{cm}^{-1}$  in DI water, or  $\epsilon_{490} = 8.0 \times 10^4 \text{ L} \cdot \text{mol}^{-1} \cdot \text{cm}^{-1}$  in 0.1M borate buffer pH = 9.3, respectively. The protein content was determined using the BCA assay following correction of the polymer content;

<sup>b)</sup> The weight-average molecular weight ( $M_w$ ) was calculated from chemical composition and size exclusion chromatography. Polymer precursors (aminolyzed with 1-amino-2-propanol) were used for the molecular weight determination of the HPMA copolymer chains. An FPLC system equipped with a Superose 6 column in 0.01M Tris buffer (pH = 8.0) containing 30% CH<sub>3</sub>CN was used. The column was calibrated with poly HPMA fractions.

**Table 3**

Cytotoxicity of free drugs and HPMA copolymer/drug conjugates in A2780 and A2780/AD cells in vitro.

Number	Conjugate	IC <sub>50</sub> [10 <sup>-6</sup> mol L <sup>-1</sup> ]		Cell-associated Mce <sub>6</sub> <sup>a)</sup> (A2780/AD) [10 <sup>-9</sup> mol L <sup>-1</sup> ]
		A2780	A2780/AD	
	free Mce <sub>6</sub>	1.7 ± 0.4	3.9 ± 0.6	49.1 ± 16.2
1	P-(G-Mce <sub>6</sub> )	96.0 ± 14.4	90.4 ± 12.2	314.2 ± 126.3
2	P-(GG-Mce <sub>6</sub> )	148.7 ± 15.3	155.1 ± 19.8	527.6 ± 109.1
3	P-(GG-Mce <sub>6</sub> )-mAb	n.d.	48.4 ± 18.0	299.2 ± 133.7
4	P-(GFLG-Mce <sub>6</sub> )	4.9 ± 0.4	6.8 ± 1.0	70.4 ± 11.4
5	P-(GFLG-Mce <sub>6</sub> )-mAb	18.9 ± 6.8	41.2 ± 6.9	213.4 ± 54.3
	free DOX	0.008 ± 0.003	9.5 ± 4.0	NA
6	P-(GG-DOX)	7.1 ± 3.2	190.3 ± 68.5	NA
7	P-(GG-DOX)-mAb	17.7 ± 2.1	45.5 ± 6.6	NA
8	P-(GFLG-DOX)	5.2 ± 2.1	108.2 ± 28.5	NA
9	P-(GFLG-DOX)-mAb	8.9 ± 3.6	13.7 ± 2.9	NA

<sup>a)</sup> Studies were conducted with the previously determined IC<sub>50</sub> dose for free Mce<sub>6</sub> or HPMA copolymer/Mce<sub>6</sub> conjugates.